LINC01094 Upregulates LIN28B Expression by Sponging miR-577 to Promote Pancreatic Cancer Proliferation and Metastasis

Chen Luo (✉ 278894094@qq.com)
  Nanchang University Second Affiliated Hospital

Kang Lin
  Nanchang University Second Affiliated Hospital

Cegui Hu
  Nanchang University Second Affiliated Hospital

Xiaojian Zhu
  Nanchang University Second Affiliated Hospital

Jinfeng Zhu
  Nanchang University Second Affiliated Hospital

Zhengming Zhu
  Nanchang University Second Affiliated Hospital

Research

Abstract

Background: The leading cause of death in pancreatic cancer (PC) patients is the progression of cancer metastasis. Long non-coding RNAs (lncRNAs) play an important role in regulating cancers, however its molecular basis in pancreatic cancer (PC) remains to be explored.

Methods: In this study, bioinformatics methods are used to predict the potential pairs of lncRNAs in PC. The clinical significance of LINC01094 are determined by qRT-PCR and explored its correlation with clinicopathological parameters. The biological functions and potential mechanisms of LINC01094 in PC progression are studied *in vivo* and *in vitro*.

Results: We observe that LINC01094 is markedly overexpressed in pancreatic tumors and is associated with poorer prognosis. Downregulation of LINC01094 decreases PC cell invasion and inhibits tumorigenesis and metastasis in mouse xenografts. LINC01094 acts as a sponge for miR-577, sequestering it and derepressing the expression of its endogenous target the RNA-binding protein lin-28 homolog B (LIN28B).

Conclusions: Overall, LINC01094 upregulates LIN28B by sponging miR-577, thereby promoting PC proliferation and metastasis. This indicates that LINC01094 can be regarded as a new biomarker or therapeutic target for the treatment of PC.

Introduction

Pancreatic cancer (PC) is one of the most frequently diagnosed cancers and the fourth leading cause of cancer related death in the United States [1]. Although the diagnosis and treatment of PC have made remarkable progress, the majority of PC patients have relapse due to local infiltration or extensive metastasis [2–5]. Therefore, understanding the molecular regulation mechanism involved in the proliferation and metastasis of PC cells is urgently needed in the treatment of PC.

Long non-coding RNAs (lncRNAs) are a kind of RNA with length longer than 200 nucleotides and which have no function of protein coding [6–9]. In recent years, lncRNAs have been found to play crucial roles in the recurrence, metastasis, and chemotherapy resistance of tumors [10–13]. For example, oncogenes RAS and MYC can promote tumorigenesis through lncRNA Orilnc1 and DANCR, respectively [14, 15]. Several kinds of lncRNA have been involved in metastasis of cancers. In PC, the expression of lncRNAs are often maladjusted, for example lncRNA HULC is abnormally increased in PC, and its high expression is significantly related to metastasis and vascular invasion of PC [16]. In addition, lncRNA PVT1 upregulates the progression and glycolysis of PC cells by regulating mir-519d-3p and HIF1α, and LINC00657 acts as a miR-433 sponge to enhance the malignancy of pancreatic ductal adenocarcinoma [17, 18]. Although lncRNA plays a decisive role in PC, the study of LINC01094 in PC has not been reported, and the interaction between LINC01094 and miRNA remains unclear. Previous studies have shown that LINC01094, as miR-224-5p competitive endogenous ribonucleic acid (ceRNA), is an important anti-cancer microribonucleic acid (miRNA) that enhances the pathogenesis of renal cell carcinoma [19]. MiRNAs have

been considered as crucial modulators in tumors, Zhang et al. found that miR-577 to be correlated with the formation and progression in glioblastoma and liver cancers [20, 21].

In the current study, a novel human lncRNA is identified, named LINC01094. Interestingly, LINC01094 is remarkably increased in PC, which is related to poor prognosis among PC patients. In addition, we found that LINC01094 down-regulation inhibits PC proliferation and metastasis by up-regulating miR-577, a potential tumor suppressor in PC. Mechanistically, LINC01094 is the sponge of miR-577, which promotes LIN28B expression, thus promoting proliferation and metastasis of PC. Our findings provided a new insight for exploring a potential therapeutic strategy for the treatment of PC.

Materials And Methods

Bioinformatics analysis

GSE7189, GSE15471, GSE102238-A, and GSE102238-B datasets were retrieved from TCGA dataset (http://gepia.cancer-pku.cn/index.html). The nearby genes of LINC01094 were searched from UCSC (http://genome.ucsc.edu/). The miRNAs that had complementary base-paring with LINC01094 were predicted by using starBase database (http://starbase.sysu.edu.cn/).

Samples

The PC tissues and pancreatic carcinomas of 91 patients with PC diagnosed in the second affiliated Hospital of Nanchang University from April 2016 to September 2020 were collected. The experiments were undertaken with the understanding and written consent of each subject and the study methodologies conformed to the standards set by the Declaration of Helsinki. This research was approved by the Ethics Committee of the Second Affiliated Hospital of Nanchang University.

Cell culture

Five human PC cell lines (PANC-1, ASPC-1, BXPC-3, CFPAC-3, SW1990) and one normal immortalized pancreatic cell line HPDE6-C7 were purchased from the Shanghai Institute of Cells of the Chinese Academy of Sciences. Cell Bank using short tandem repeats was used to identify all these cells. The cells were routinely cultured in DMEM medium containing 10% fetal bovine serum (FBS, Gibco) at (37°C, 5% CO_2).

Cell transfection

The LINC01094-overexpressing and shLINC01094-expressing plasmids, the miR-577 mimic (miR-577) and negative control (miR-NC) were designed and synthesized by GenePharma (Suzhou, China). Cells transfected with the empty vector were designated or treated as control (named as vector). The LINC01094 specific small interfering RNA (siRNA) and negative control (siNC) were purchased from GenePharma (Shanghai, China). Cell transfection was conducted by use of Lipofectamine 3000 (Invitrogen CA, USA). The plasmids and reagents used are described in the Supplementary Table 1.

Quantitative real-time PCR (qRT-PCR)

Total RNA was extracted from tissue or cultured cells using RNAiso Plus (Takara, Japan), then the RNA was inversely transcribed into cDNA, and was used for PCR amplification. The results were analyzed by $2^{-\triangle\triangle Ct}$ method. All the primers are in Supplementary Table 1.

Fluorescence in situ hybridization (FISH)

The FISH Kit was purchased from RiboBio. LINC01094 probes were designed by RiboBio. Transfected PC cells were fixed in 4% paraformaldehyde for 15 minutes, then were permeabilized in PBS containing 0.5% Triton X-100 and prehybridized in hybridization buffer (8 ul 25% dextran sulfate (DS), 20 ul 20x SSC (175.3 g NaCl, 88.2 g sodium citrate, 1000 ml H_2O), and 5 ul deionized formamide). Next, cells were further incubated with 50 nM of the probe in hybridization buffer at 4 °C overnight. The next day, cells were washed with PBS and counterstained with 4', 6-diamidino-2-phenylindole (DAPI). All images were analyzed on a confocal laser scanning microscope (Leica Microsystems, Mannheim, Germany). The FISH probe sequences are shown as follows: LINC01094: 5'-TAGATTTAACTGCCTAACTAACGATGAAGC-3'.

Western blotting

As mentioned earlier, western blotting analysis was performed [22]. The antibodies in this study are as follows: rabbit antibody LIN28B (1:5,00, ab46020, Abcam), rabbit antibody PCNA (1:1,000, ab92552, Abcam), rabbit antibody MMP9 (1:1,000, ab137867, Abcam) and mouse antibody GAPDH (1:1,000, ab9484, Abcam).

Immunohistochemistry analysis

IHC analysis of LIN28B, PCNA, MMP9 procedures were performed as described previously [23]. Antibodies used were as follows: rabbit antibody PCNA (1:2,00, ab92552, Abcam), rabbit antibody LIN28B (1:2,00, ab262858, Abcam), rabbit antibody MMP9 (1:2,00, ab137867, Abcam).

Colony formation assay

Transfected PC cells were seeded in 6 well plates with a total of 500 cells per well. After 2 weeks of incubation, they were fixed with 4% paraformaldehyde, then incubated with crystal violet for 15 minutes, and counted under the microscope.

5-Ethynyl-2'-deoxyuridine (EdU) assay

The cells were incubated with 5-Ethynyl-2'-deoxyuridine (EdU; Ribobio) for 5 hours. After three rinses with PBS, the cells were treated with 300 ml of 1 × Apollo reaction cocktail for 30 min. The DNA content of the cells in each well was then stained with 100 ml of Hoechst 33342 (5 mg/ml) for 30 minutes. Subsequently, the cells were visualised under a fluorescence microscope.

Wound healing assay

The wound healing rate was detected by scratch test to evaluate the ability of cell migration, which was briefly described as follows: cells were inoculated in a 6-well plate to form a monolayer and scratched with a sterile pipette (200 µl). Loose cell fragments were washed with PBS, and the remaining cells were cultured for 0 hours and 48 hours. Then the wound images were taken by microscope, and migration distance of the monolayer growth edge at 24 h after injury was observed, and the wound healing rate was calculated.

Transswell assay

Three groups of cells were inoculated on the transwell chamber with 1×10^4 cells per group. After 24 hours of culture, formaldehyde was fixed through the cells under the ependyma, and the staining solution was 0.2% crystal violet solution and enumerated it under the microscope.

Subcellular fractionation assay

PANC-1 and ASPC-1 cell lines were collected in cell fractionation buffer using PARIS™ Kit (Invitrogen, USA). PBS washed the cell fragments. Cell fractionation buffer was used to place the cell lysates and centrifuged. The isolated RNA was used for PCR amplification. The cytoplasmic and nuclear fractionation indicators used were GAPDH and U6, respectively.

Luciferase reporter gene assay

The wild-type LINC01094 (Wt-LINC01094) and the wild-type LIN28B (Wt-LIN28B) with predicted binding site of miR-577 and the promoter region of Mut-LINC01094 and Mut-LIN28B were synthesized and cloned into luciferase reporter vector pGL3 (Promega, Madison, WI). The PC cells were co-transfected with corresponding reporter plasmids and miR-577 mimic or NC mimic by Lipofectamine 3000 and were detected by the double luciferase report method.

Immunoprecipitation of RNA binding protein (RIP)

Resulting transfected cells lysed with RIPA buffer, centrifuged at 14, 000 rpm for 15 minutes, then incubated overnight at 4 °C, with shaking prior to addition of 10 µl of beads and 2 µl of Ago2 antibody. The mixture was rinsed twice using a lysis buffer, and Trizol reagent (Invitrogen) was used to extract RNA from the lysed cells.

In vivo tumor growth and metastasis assay

The 6- to 8-week-old nude male mice were purchased from the Institute of Model Zoology, Nanjing University. All experiments were performed in accordance with the NIH guidelines for the humane care and use of laboratory animals and were approved by the Institutional Animal Care and Use Committee at Nanchang University. The cell concentration was adjusted to 1×10^6 cells/ml. After the skin of the back of nude mice was disinfected with 75% alcohol, 0.2 ml cell suspension was injected into the back and intrasplenical region of nude mice to establish the model of ectopic tumor formation of PC cells in nude mice. The general health status and tumor growth of nude mice were observed regularly, and the volume and weight of the transplanted tumor were recorded.

Statistical analysis

SPSS 22.0 software was used to statistically process the data and all results were displayed as means ± standard deviation (SD). Student's t-test was used for comparison between two groups while more than two groups were analyzed by one-way analysis of variance (ANOVA) and post-hoc test to correct for multilple comparisons. Spearman correlation analysis was used for correlation, $p < 0.05$ was set as threshold for statistical significance.

Results

LINC01094 is upregulated in PC and is associated with poor prognosis

To identify the abnormally expressed lncRNAs in PC, we used the BLAST program, through U133PLUS2.0 technology to compare the lncRNA database with the GEO database and selected 4 microarray data sets (GSE7189, GSE15471, GSE102238-A and GSE102238-B), (Fig. 1A, Supplementary Fig. 4, Fig. 5 and Fig. 6). Three lncRNAs probes were consistent in all four datasets (Fig. 1B). LINC01094 was one of the most significantly upregulated lncRNA in the four datasets (Fig. 1C, **$p < 0.01$). In addition, qRT-PCR analysis showed that LINC01094 expression was higher in PC tissues than in non-tumor tissues from TCGA database (Fig. 1D, **$p < 0.01$). Moreover, the level of LINC01094 in advanced PC (stage III and IV) was upregulated compared with early stage PC (stage I and II) (Fig. 1E, **$p < 0.01$). Next, we evaluated the relationship between LINC01094 level and clinicopathological features of PC (Table 1). This analysis indicated that the high level of LINC01094 correlated with tumor size (***$p < 0.001$), lymph node metastasis (***$p < 0.001$), venous invasion (***$p < 0.001$), and TNM stage (***$p < 0.001$). Kaplan-Meier survival analysis revealed that high level of LINC01094 was associated with the poor survival rate of patients with PC from TCGA database (Fig. 1F, $p = 0.00071$). In addition, univariate analysis indicated that tumor size, lymphatic metastasis, venous invasion, TNM classification and LINC01094 expression were noteworthy predictors of overall survival in PC patients (all $p < 0.01$, Table 2). Multivariate analysis showed that LINC01094 was an independent protective predictor of overall survival ($p < 0.01$, Table 2). In addition, tumor size, lymphatic metastasis, venous invasion, TNM classification also were independent risk predictors of overall survival in PC patients ($p < 0.01$, Table 2). Taken together, these results indicated that high LINC01094 expression is associated with poor prognosis, highlighting the potential of LINC01094 as an independent prognostic marker in PC.

Table 1

The correlation between the clinicopathological characteristics and LINC01094 expression in 91 PC patients.

Characteristics	No. of patients	LINC01094 expression		P**
		Low n = 33	High n = 58	
Age (year)	49	19	30	0.59
< 60	42	14	28	0.482
≥ 60	37	15	22	0.011*
Gender	54	18	36	0.776
Female	57	15	42	
Male	34	18	16	
Tumor size (mm)	45	17	28	
<30	46	16	30	
≥ 30				
Location				
Head/neck				
Body/tail				
Lymphatic metastasis				
Positive	53	12	41	
Negative	38	21	17	0.001**
Distant metastasis				
Positive	41	9	32	
Negative	50	24	26	0.01*
TNM stage				
I/II	41	20	21	
III/IV	50	13	37	0.025*

Table 2

Univariate and multivariate analyses of survival in 91 PC patients (Cox proportional hazards regression model)

Variables	Univariate analysis			Multivariate analysis		
	HR	95%CI	P value	HR	95%CI	P value
Age (≥ 60 vs ᐸ60)	1.304	0.763–2.228	0.331	—	—	—
Gender (Male vs Female)	1.127	0.646–1.966	0.673	—	—	—
Tumor size (cm) (≥ 3 vs < 3)	2.622	1.516–4.535	0.001**	2.108	1.147–3.874	0.016**
Location head/neck vs Body/tail	1.459	0.854–2.492	0.167	—	—	—
Lymphatic metastasis (Positive vs Negative)	7.992	3.809–16.77	< 0.001**	6.313	2.60-15.327	0.001**
Distant metastasis (Positive vs Negative)	6.346	2.718–14.816	< 0.001**	2.496	1.336–4.664	0.004**
TNM staging (I/II vs III/IV)	6.58	3.604–12.013	< 0.001**	3.039	1.501–6.151	0.002**
LINC01094 expression (High vs Low)	5.181	2.544–10.552	< 0.001**	3.644	1.439–9.223	0.006**

LINC01094 promotes the proliferation of PC cells in vitro

Next, we analyzed LINC01094 expression in a normal pancreatic cell (HPDE6-C7) and PC cell lines (CFPAC-1, BXPC-3, ASPC-1, PANC-1, and SW1990). The results showed that LINC01094 expression in PC cells was higher than in normal cells (Fig. 2A). Then, ASPC-1 and PANC-1 cells with the high level of LINC01094 were selected to transfect siRNA-LINC01094#1 (siLINC01094#1 group), siRNA- LINC01094#2 (siLINC01094#2 group), and negative control sequence (siNC), (Fig. 2B). Down-regulation of LINC01094 decreased the colony formation capacity and cell growth of PC (Fig. 2C and D, **p < 0.01). In contrast, overexpression of LINC01094 significantly enhanced the proliferation of CFPAC-1 cells (Supplementary Fig. S2B and C, **p < 0.01). Western blot analysis showed that silencing of LINC01094 in PANC-1 and ASPC-1 cells inhibited PCNA expression, factor known to promote cell proliferation (Fig. 2C) while overexpression of LINC01094 did the opposite (Supplementary Fig. S2F, **p < 0.01). Taken together, these datasets suggest that LINC01094 may promote PC progression.

LINC01094 promotes PC cells metastasis in vitro

To explore the function of LINC01094 in PC cells metastasis. We designed wound healing and transwell experiments in PANC-1 and ASPC-1 cells. The results showed that down-regulation of LINC01094 decreased the migration and invasion ability of PC cells and suggested that growth and survival of PANC-1 cells was affected more than that of ASPC-1 cells (Fig. 3A and B, **p < 0.01). However, overexpression of LINC01094 significantly increased the migration and invasion ability of CFPAC-1 cells (Supplementary Fig. S2D and E, **p < 0.01). Western blot analysis showed that silencing of LINC01094 in PANC-1 and ASPC-1 cells inhibited MMP9 expression, which promotes cell metastasis (Fig. 3C), while overexpression of LINC01094 enhanced MMP9 (Supplementary Fig. S2F, **p < 0.01). Taken together, these data suggest that LINC01094 may promote PC progression.

LINC01094 acts as miRNA sponge for miR-577

LncRNAs could recruit miRNAs to function as competing endogenous RNAs (ceRNAs) during oncogenesis [24]. To verify whether LINC01094 had a similar function in PC cells, lncRNA subcellular localization predictor (lncLocator, http://www.csbio.sjtu.edu.cn/bioinf/lncLocator/) was used to predict its localization in cells and subcellular fractionation was performed for confirmation. Data showed that LINC01094 was mainly localized to the cytoplasm (Fig. 4A and B). In addition, fluorescence in situ hybridization (FISH) results suggested that LINC01094 mainly located in the cytoplasm (Fig. 4C), indicating that LINC01094 might regulate target protein expression at the posttranscriptional level. Next, we used the bioinformatics databases starBase (http://starbase.sysu.edu.cn/) to predict the potential miRNAs (Supplementary Table 2). According to the predicted result, there were three miRNAs (miR-577, miR-330-3p and miR-545-3p) for whom LINC01094 contained multiple binding sites. QRT-PCR analysis was used to detect the expression of the three miRNAs in PC cells down-regulated by shLINC01094 and up-regulated by LINC01094, and only miR-577 changed (Fig. 4D, **p < 0.01). In addition, LINC01094 expression did not change after knockdown of miR-577 (Fig. 4E, N.S p > 0.05). Therefore, we regarded miR-577 as the main candidate for further research. To verify the direct binding of LINC01094 and miR-577 at the endogenous level, luciferase reporter analysis was conducted, which included LINC01094 binding sites of wild-type (Wt) or mutant (Mut) (Fig. 4F, **p < 0.01). The results indicated that miR-577/mimic decreased the luciferase activity of Wt-LINC01094 reporter vector, however the luciferase activity of Mut-LINC01094 reporter vector did not decrease (Fig. 4G, **p < 0.01). It was well known that miRNAs bound to its target and caused translation inhibition and RNA degradation in an Ago2 dependent manner [25]. To further validate the potential binding of LINC01094 to miR-577, an RNA Immunoprecipitation (RIP) assay using an anti-Ago2 antibody was performed. The data exhibited that both LINC01094 and miR-577 were obviously enriched in Ago2 complex (Fig. 4H, **p < 0.01), which identified that LINC01094 might act as a ceRNA to regulate miR-577. In addition, we found that the expression of miR-577 in a normal pancreatic cells and adjacent normal tissues were higher than that in PC cells and PC tissues (Fig. 4I and J, **p < 0.01), and negatively correlated with LINC01094 (Fig. 4K, r =-0.6024, **p < 0.01). Moreover, low miR-577 expression predicted a poor prognosis in PC patient (Fig. 4L, p = 0.0017).

LIN28B is a downstream target of miR-577

To explore the down-stream target of miR-577, we analyzed five miRNA datasets and then looked for the potential miR-577 target genes in all of them (Fig. 5A). Also, we analyzed miR-577 expression in a normal pancreatic cell (HPDE6-C7) and PC cell lines (CFPAC-1, BXPC-3, ASPC-1, PANC-1, and SW1990). The results showed that miR-577 expression in PANC-1 cells was lower than in other cells and miR-577 expression in CFPAC-1 cells was higher (Fig. 4I, **p < 0.01). So PANC-1 cells with the low level of miR-577 were selected to transfect miR-577/inhibitor, and CFPAC-1 cells with the high level of miR-577 were selected to transfect miR-577/mimic, followed by qRT-PCR analysis of the four targets where we found that only LIN28B changed (Fig. 5B). To verify the direct binding of LIN28B and miR-577 at the endogenous level, luciferase reporter analysis was designed, which included LIN28B binding sites of Wt or Mut syndrome. The results indicated that miR-577/mimic decreased the luciferase activity of Wt-LIN28B reporter vector, however the luciferase activity of Mut-LIN28B reporter vector did not decrease (Fig. 5C and D). To further illustrate the potential interaction between LIN28B and miR-577, miR-577 mimic was transfected into PANC-1 cells, followed with a qRT-PCR and western blot analysis. The results showed that LIN28B mRNA and protein levels were significantly down-regulated (Fig. 5E and F, **p < 0.01). Moreover, western blot analysis showed that silencing of miR-577 in PANC-1 cells promoted MMP9, PCNA and LIN28B expression, factors known to promote cell proliferation and metastasis, while overexpression of miR-577 inhibited their expression (Fig. 5F, **p < 0.01). Plate cloning and EdU assays showed that miR-577 overexpression could significantly decrease colony formation and growth. In contrast silencing of miR-577 promoted colony formation and growth in CFPAC-1 cells (Fig. 5G and H, **p < 0.01). Wound healing and transwell assays also showed that miR-577 overexpression could significantly decrease the ability of metastasis in PANC-1 cells, however, down-regulation of miR-577 had the opposite effect in CFPAC-1 cells (Fig. 5I and J, **p < 0.01). Additionally, we found that the expression of LIN28B was highly expressed in PC tissues compared with non-tumor tissues (Fig. 5K and L, **p < 0.01), and negatively correlated with LINC01094 (Fig. 5M, r = 0.4918, **p < 0.01).

LINC01094 acts as a sponge of miR-577 to upregulate LIN28B expression

Since LINC01094 could inhibit miR-577 expression, we then determined whether LINC10094 could affect the expression of LIN28B through competitive binding with miR-577. To this end, rescue experiments were designed using miR-577 inhibitor and mimic. As expected, western blot assays demonstrated that knockdown of LINC01094 decreased the protein levels of LIN28B, PCNA, and MMP9 in PANC-1 cell, while upregulation of LINC01094 enhanced the levels of LIN28B, PCNA, and MMP9 in CFPAC-1 cell (Fig. 6A, **p < 0.01). Simultaneously, the effects caused by silencing or overexpressing LINC01094 were reversed by miR-577 mimic or inhibitor, respectively (Fig. 6A, **p < 0.01). Moreover, plate cloning and EdU assays showed that the miR-577 inhibitor reversed the proliferation, migration and invasion suppressing effects induced by knockdown of LINC01094 in PANC-1 cells, whereas miR-577 mimic counter-acted the promoting effects induced by overexpression of LINC01094 in CFPAC-1 cells by colony formation, EDU, wound healing and transwell assays (Fig. 6B and E, **p < 0.01). To investigate whether LINC01094 exerts

tumor-promoting functions in PC by modulating the miR-577/LIN28B axis, we then checked the effects of LIN28B on LINC01094-induced cell proliferation and metastasis by colony formation, EDU, wound healing and transwell assays (Supplementary Fig. 3B-E, **p < 0.01) and observed that LIN28B knockdown blocked the LINC00194-induced the proliferation, migration and invasion of PC cells. Next, western blotting was performed to investigate whether LIN28B affect MMP9 and PCNA levels in the context of LINC01094-driven cell proliferation and metastasis. Results showed that LIN28B knockdown significantly reversed the effects of LINC01094 overexpression on MMP9 and PCNA expression (Supplementary Fig. 3A, **p < 0.01). Collectively, these data demonstrated that LINC01094 served as a ceRNA for miR-577 to regulate LIN28B expression, thus leading to the progression and development of PC.

Silencing of LINC01094 suppresses the proliferation and metastasis of PC cells in vivo.

In order to verify whether the LINC01094 affected the growth of PC *in vivo*, we constructed LINC01094 stable knockdown in PANC-1 cells using a lentivirus carrying shRNA (shLINC01094) into BALB/c-free nude (male, 6−8 weeks). Compared with the shNC, the tumor growth and body weight of the shLINC01094 was significantly reduced (Fig. 7A and C, **p < 0.01). These subcutaneous tumor tissues were further utilized for western blot assays. And results of western blot and IHC assays showed the expression of LIN28B, PCNA and MMP9 was downregulated in the shLINC01094 group compared to the shNC group (Fig. 7D and F, **p < 0.01). Moreover, qRT-PCR analysis of miR-577 have be done in these subcutaneous tumor tissues. The result showed that the expression of miR-577 was upregulated in the shLINC01094 group compared to the shNC group (in Fig. 7E, **p < 0.01). To investigate whether LINC01094 affected the invasion and migration of PC *in vivo*, we constructed LINC01094 stable knock-down in PANC-1 cells using a lentivirus carrying shRNA (shLINC01094) into BALB/c-free male nude mice. Compared to the shNC, the metastatic nodules decreased in liver and lung (Fig. 7F and G, **p < 0.01). Furthermore, mice of the PANC-1-shLINC01094) group survived longer than controls (Fig. 7I, p = 0.00126). These data demonstrated that LINC01094 can promote PC cell proliferation and metastasis in *vivo.*

Discussion

Recent years, more and more studies report that lncRNAs are associated with the progression of cancers [26−28]. For example, in PC, lncRNA PLACT1 promoted growth and metastasis of pancreatic ductal carcinoma cells via the IκBα/E2F1 axis [29]. Another lncRNA, ENSGO0000254041.1, promoted pancreatic ductal carcinoma cells invasion, which was related to the poor prognosis of patients [30]. LINC01094 was first described in renal cell carcinoma and promoted the development of clear cell renal carcinoma through miR-224-5p/CHSY1 axis [19]. However, the function of LINC01094 in PC had not been well studied. In this study, we screened the TGCA database and bioinformatics analysis of GEPIA (Gene Expression Profiling Interactive Analysis) data showed that a new type of lncRNA, LINC01094, was found to have high expression in PC tissues, while associating with poor prognosis and diminished survival time. In addition, knock-down of LINC01094 inhibited PC cells growth and metastasis ability.

Increasing evidence showed that there were extensive interaction networks involving ceRNA, in which lncRNA could regulate the target RNA by binding to the target RNA and titrating from the binding site on the protein coding messenger [31, 32]. Target molecules regulated mutual expression by competing to bind miRNA's response element (MRE) [33]. Evidence suggested that the ceRNA regulatory model had been validated in other cancers. For example, lncRNA MIR31HG inhibited the proliferation and metastasis of PC and caused sponge miR-575 to slightly regulate the expression of ST7L [34]. LINC00473 played a key role, because ceRNA regulated MAPK1 expression by turning miR-198 into a sponge [35]. Bioinformatics analysis, fluorescence reporter gene detection and RIP analysis indicated that miR-577 was the target of LINC01094. Based on the previous research and functional analysis of LINC01094, we chosed miR-577 for further research. The results showed that knocking down LINC01094 in PC cells could upregulate the expression of miR-577, and the LINC01094 expression did not change after knocking down miR-577. Then we used bioinformatics analysis to predict miR-577 targets and LIN28B was the most significantly downregulated target gene of miR-577. Lin 28 homolog B (LIN28B), an RNA-binding protein, functions as an oncogene and is a potential therapeutic target for cancer [36, 37]. Previous reports have proved that LIN28B is target of miR-30a-5p and upregulation of LIN28B promotes tumor growth in breast cancers [38]. Moreover, miR-577 acts as a suppressor in many cancers, including glioblastoma and liver cancers [20, 21]. In this study, our findings indicated that miR-577 inhibition increased pancreatic cancer growth and metastasis. Moreover, recovery assay showed that LINC01094 affected PC cells growth and metastasis in a partially miR-577 dependent manner *in vitro*. To sum up, these data strongly indicate that miR-577 is the real miRNA targeting LINC01094. Our research showed that the suppression of PC cells proliferation and metastasis attained by LINC01094 knockdown was reversed by miR-577 inhibition, and LINC01094 was correlated with miR-577 and LIN28B in PC tissues. These results suggest that LINC01094 could be used as a ceRNA to upregulate LIN28B expression in a miR-577-dependent manner.

Conclusion

In summary, we showed for the first time that LINC01094 exhibited its oncogenic function in PC through sponging miR-577 to mediate LIN28B expression. Thus, this study revealed a novel oncogenic pathway in PC tumorigenesis, which will provide a new thought in exploring the novel diagnostic or therapeutic biomarker for PC.

Abbreviations

PC: Pancreatic cancer; LIN28B: RNA-binding protein lin-28 homolog B; LncRNAs: Long non-coding RNAs; DAPI: 4', 6-diamidino-2-phenylindole; EdU: 5-Ethynyl-2'-deoxyuridine; qRT-PCR: quantitative real-time polymerase chain reaction; RIP: Immunoprecipitation of RNA binding protein; FISH: Fluorescence in situ hybridization; 3'-UTR: 3'-untranslated region; SD: standard deviation; ANOVA: One-way analysis of variance; miRNA: microribonucleic acid: ceRNA: Competing endogenous RNA; shRNA: Short hairpin RNA;

Wt: Wide type; Mut: Mutated type; N.S: no significance, GEPIA: Gene Expression Profiling Interactive Analysis.

Declarations

Ethics approval and consent to participate

The Ethics Committee of the Second Affiliated Hospital of Nanchang University reviewed and approved all research procedures involving human or animal participants. All patients expressed informed consent.

Consent for publication

Not applicable.

Availability of data and materials

All the data and materials supporting the conclusions were included in the main paper.

Competing interests

The authors declare that they have no competing interests.

Founding

Authors' contributions

CL and ZZ designed the study. KL and XZ provided suggestions for the project. CL and ZZ performed the primary experiments and wrote the manuscript. KL, XZ and JZ analyzed the data. CL, CH and JZ revised the figures and tables. KL, XZ and JZ collected the tissue samples and clinical datas of PC patients.

Acknowledgements

Authors details

[1]Department of General Surgery, Second Affiliated Hospital of Nanchang University, Nanchang, China.

[2]Jiangxi Province Medical College of Nanchang University, Nanchang, China.

References

1. Jooste V, Dejardin O, Bouvier V, Arveux P, Maynadie M, Launoy G, et al. Pancreatic cancer: Wait times from presentation to treatment and survival in a population-based study. Int J Cancer. 2016;139(5):1073–80.

2. Puleo F, Marechal R, Demetter P, Bali MA, Calomme A, Closset J, et al. New challenges in perioperative management of pancreatic cancer. World journal of gastroenterology. 2015;21(8):2281–93.

3. Garrido-Laguna I, Hidalgo M. Pancreatic cancer: from state-of-the-art treatments to promising novel therapies. Nature reviews Clinical oncology. 2015;12(6):319–34.

4. Siegel RL, Miller KD, Jemal A. Cancer statistics. 2018. CA: a cancer journal for clinicians. 2018;68(1):7–30.

5. Campbell PJ, Yachida S, Mudie LJ, Stephens PJ, Pleasance ED, Stebbings LA, et al. The patterns and dynamics of genomic instability in metastatic pancreatic cancer. Nature. 2010;467(7319):1109–13.

6. Batista PJ, Chang HY. Long noncoding RNAs: cellular address codes in development and disease. Cell. 2013;152(6):1298–307.

7. Guttman M, Amit I, Garber M, French C, Lin MF, Feldser D, et al. Chromatin signature reveals over a thousand highly conserved large non-coding RNAs in mammals. Nature. 2009;458(7235):223–7.

8. Nagano T, Fraser P. No-nonsense functions for long noncoding RNAs. Cell. 2011;145(2):178–81.

9. Ponting CP, Oliver PL, Reik W. Evolution and functions of long noncoding RNAs. Cell. 2009;136(4):629–41.

10. Ulitsky I, Bartel DP. lincRNAs: genomics, evolution, and mechanisms. Cell. 2013;154(1):26–46.

11. Kallen AN, Zhou XB, Xu J, Qiao C, Ma J, Yan L, et al. The imprinted H19 lncRNA antagonizes let-7 microRNAs. Molecular cell. 2013;52(1):101–12.

12. Schmitt AM, Chang HY. Long Noncoding RNAs in Cancer Pathways. Cancer cell. 2016;29(4):452–63.

13. Chen LL. Linking Long Noncoding RNA Localization and Function. Trends Biochem Sci. 2016;41(9):761–72.

14. Zhang D, Zhang G, Hu X, Wu L, Feng Y, He S, et al. Oncogenic RAS Regulates Long Noncoding RNA Orilnc1 in Human Cancer. Cancer research. 2017;77(14):3745–57.

15. Lu Y, Hu Z, Mangala LS, Stine ZE, Hu X, Jiang D, et al. MYC Targeted Long Noncoding RNA DANCR Promotes Cancer in Part by Reducing p21 Levels. Cancer research. 2018;78(1):64–74.

16. Peng W, Gao W, Feng J. Long noncoding RNA HULC is a novel biomarker of poor prognosis in patients with pancreatic cancer. Medical oncology (Northwood, London, England). 2014;31(12):346.

17. Sun J, Zhang P, Yin T, Zhang F, Wang W. Upregulation of LncRNA PVT1 Facilitates Pancreatic Ductal Adenocarcinoma Cell Progression and Glycolysis by Regulating MiR-519d-3p and HIF-1A. J Cancer. 2020;11(9):2572–9.

18. Bi S, Wang Y, Feng H, Li Q. Long noncoding RNA LINC00657 enhances the malignancy of pancreatic ductal adenocarcinoma by acting as a competing endogenous RNA on microRNA-433 to increase PAK4 expression. Cell cycle (Georgetown Tex). 2020;19(7):801–16.

19. Jiang Y, Zhang H, Li W, Yan Y, Yao X, Gu W. FOXM1-Activated LINC01094 Promotes Clear Cell Renal Cell Carcinoma Development via MicroRNA 224-5p/CHSY1. Molecular and cellular biology. 2020;40(3).

20. Zhang W, Shen C, Li C, Yang G, Liu H, Chen X, et al. miR-577 inhibits glioblastoma tumor growth via the Wnt signaling pathway. Molecular carcinogenesis. 2016;55(5):575–85.

21. Wang LY, Li B, Jiang HH, Zhuang LW, Liu Y. Inhibition effect of miR-577 on hepatocellular carcinoma cell growth via targeting β-catenin. Asian Pacific journal of tropical medicine. 2015;8(11):923–9.

22. Li Q, Chen L, Luo C, ChenYan, Ge J, Zhu Z, et al. TAB3 upregulates PIM1 expression by directly activating the TAK1-STAT3 complex to promote colorectal cancer growth. Experimental cell research. 2020;391(1):111975.

23. Luo C, Yuan R, Chen L, Zhou W, Shen W, Qiu Y, et al. TAB3 upregulates Survivin expression to promote colorectal cancer invasion and metastasis by binding to the TAK1-TRAF6 complex. Oncotarget. 2017;8(63):106565–76.

24. Duru N, Wolfson B, Zhou Q. Mechanisms of the alternative activation of macrophages and non-coding RNAs in the development of radiation-induced lung fibrosis. World journal of biological chemistry. 2016;7(4):231–9.

25. Hammond SM. An overview of microRNAs. Adv Drug Deliv Rev. 2015;87:3–14.

26. Carlevaro-Fita J, Lanzos A, Feuerbach L, Hong C, Mas-Ponte D, Pedersen JS, et al. Cancer LncRNA Census reveals evidence for deep functional conservation of long noncoding RNAs in tumorigenesis. Communications biology. 2020;3(1):56.

27. Gutschner T, Diederichs S. The hallmarks of cancer: a long non-coding RNA point of view. RNA Biol. 2012;9(6):703–19.

28. Prensner JR, Chinnaiyan AM. The emergence of lncRNAs in cancer biology. Cancer discovery. 2011;1(5):391–407.

29. Ren X, Chen C, Luo Y, Liu M, Li Y, Zheng S, et al. lncRNA-PLACT1 sustains activation of NF-kappaB pathway through a positive feedback loop with IkappaBalpha/E2F1 axis in pancreatic cancer. Mol Cancer. 2020;19(1):35.

30. Chen B, Zhang Q, Wang X, Wang Y, Cui J, Zhuang H, et al. The lncRNA ENSG00000254041.1 promotes cell invasiveness and associates with poor prognosis of pancreatic ductal adenocarcinoma. Aging. 2020;12(4):3647–61.

31. Bayoumi AS, Sayed A, Broskova Z, Teoh JP, Wilson J, Su H, et al. Crosstalk between Long Noncoding RNAs and MicroRNAs in Health and Disease. Int J Mol Sci. 2016;17(3):356.

32. Dhanoa JK, Sethi RS, Verma R, Arora JS, Mukhopadhyay CS. Long non-coding RNA: its evolutionary relics and biological implications in mammals: a review. Journal of animal science technology. 2018;60:25.

33. Guo D, Li Y, Chen Y, Zhang D, Wang X, Lu G, et al. DANCR promotes HCC progression and regulates EMT by sponging miR-27a-3p via ROCK1/LIMK1/COFILIN1 pathway. Cell proliferation. 2019;52(4):e12628.

34. Sun Y, Jia X, Wang M, Deng Y. Long noncoding RNA MIR31HG abrogates the availability of tumor suppressor microRNA-361 for the growth of osteosarcoma. Cancer management research. 2019;11:8055–64.

35. Niu L, Zhou Y, Zhang W, Ren Y. Long noncoding RNA LINC00473 functions as a competing endogenous RNA to regulate MAPK1 expression by sponging miR-198 in breast cancer. Pathol Res Pract. 2019;215(8):152470.

36. Wang C, Gu Y, Zhang E, Zhang K, Qin N, Dai J, et al. A cancer-testis non-coding RNA LIN28B-AS1 activates driver gene LIN28B by interacting with IGF2BP1 in lung adenocarcinoma. Oncogene. 2019;38(10):1611–24.

37. Wang T, Wang G, Hao D, Liu X, Wang D, Ning N, et al. Aberrant regulation of the LIN28A/LIN28B and let-7 loop in human malignant tumors and its effects on the hallmarks of cancer. Mol Cancer. 2015;14:125.

38. Ji W, Diao YL, Qiu YR, Ge J, Cao XC, Yu Y. LINC00665 promotes breast cancer progression through regulation of the miR-379-5p/LIN28B axis. Cell death disease. 2020;11(1):16.
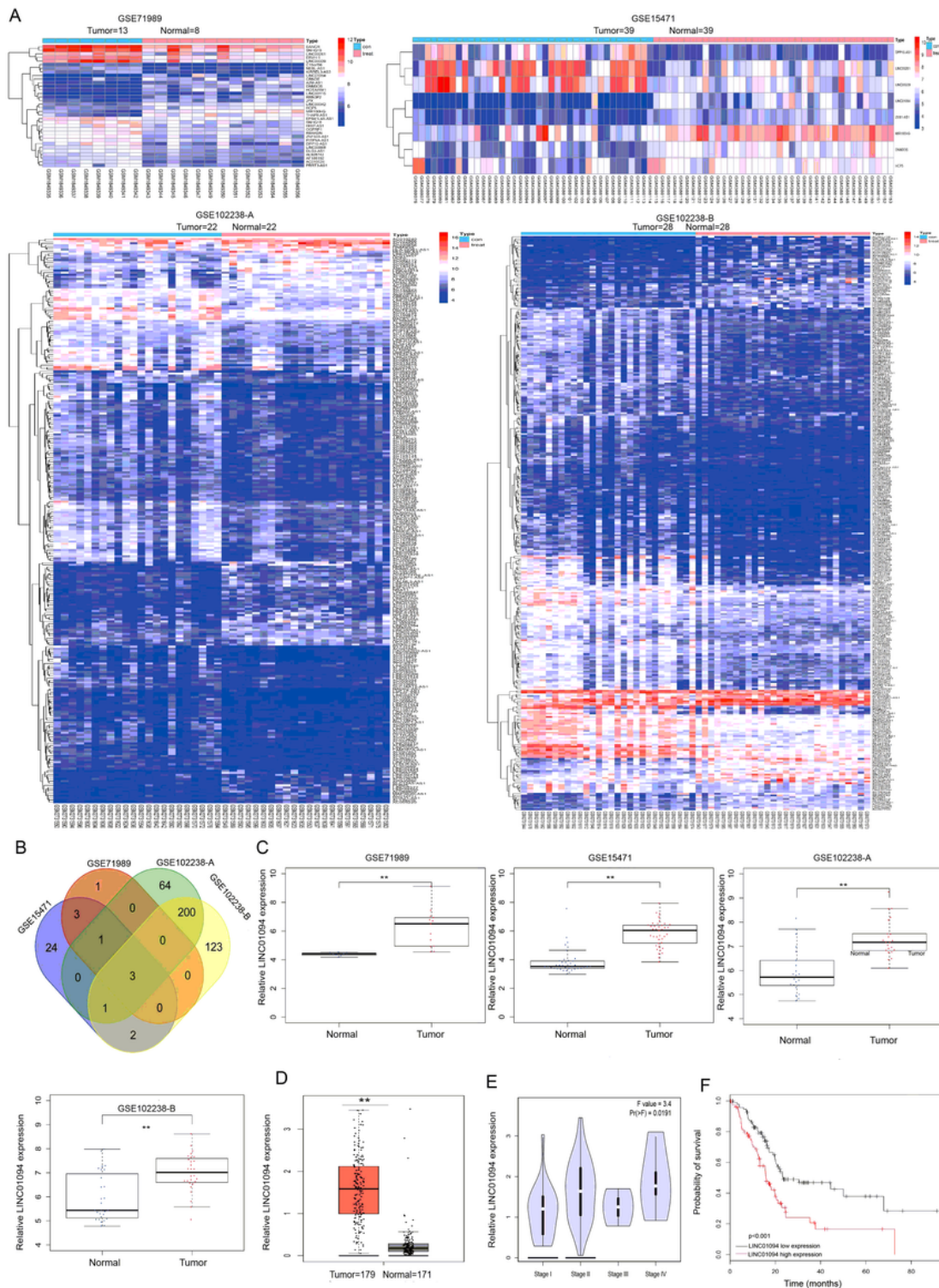
Figures

Figure 1

LINC01094 is upregulated in PC and is associated with poor prognosis. (A) Heat map showing differentially expressed lncRNA in four GEO datasets. (B) Three lncRNAs overlapping Venn diagrams represent different expressions in all four GEO datasets. (C) Relative expression of LINC01094 in four genes expression profiles of the GEO datasets. (D) The mRNA expression of LINC01094 in pancreatic cancer and normal pancreatic tissues from the TCGA database (**p<0.01). (E) Relative LINC01094

expression in PC tissues with different TNM stage (p=0.0191). (F) Kaplan-Meier analysis of survival time with LINC01094 high and low level in PC patients from TCGA database (p=0.00071, log-rank test).
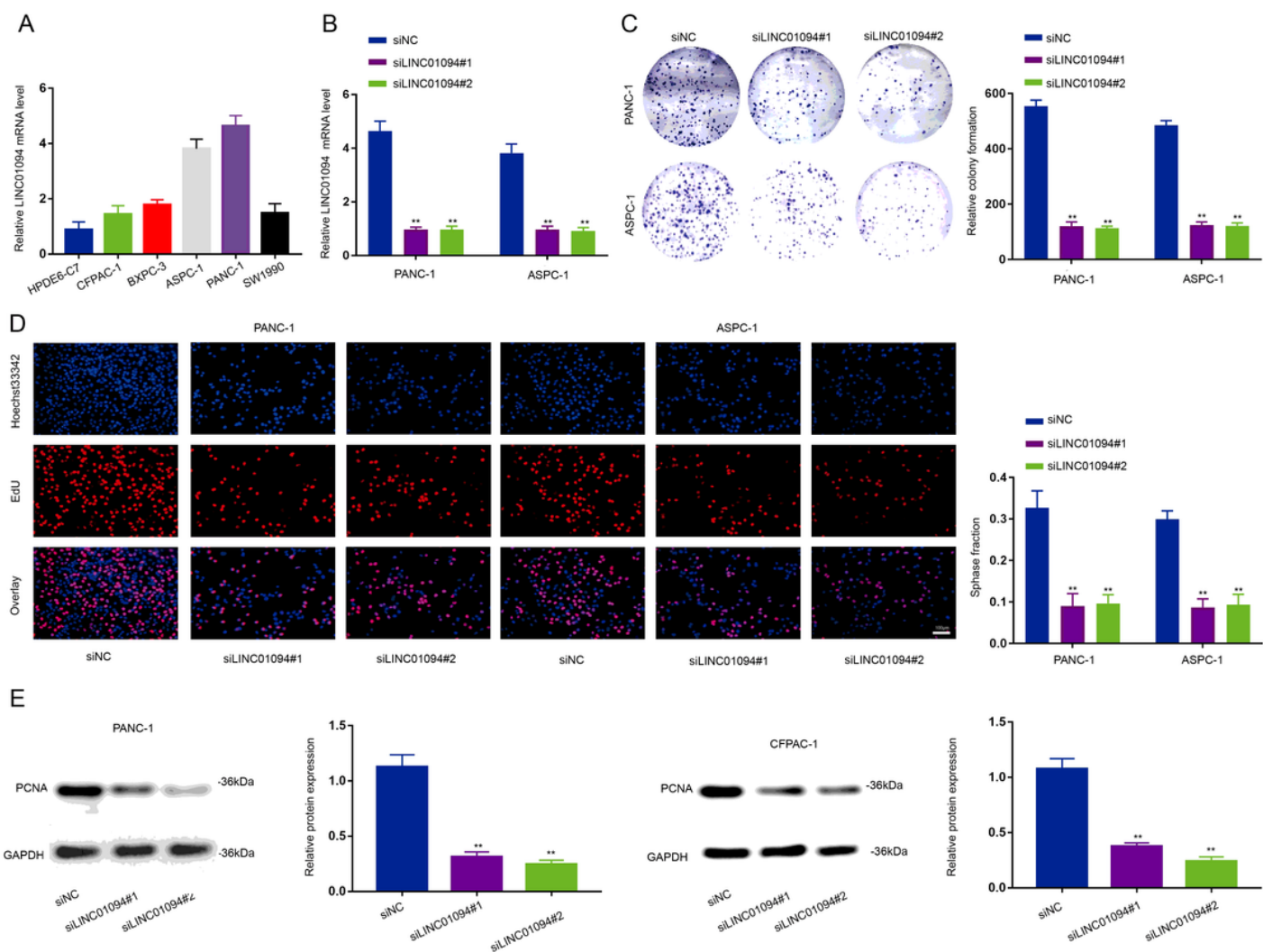

Figure 2

LINC01094 promotes the proliferation of PC cells in vitro. (A) LINC01094 mRNA expression was analyzed in PC cells and normal pancreatic cells. (B) LINC01094 mRNA expression was analyzed in PANC-1 and ASPC-1 cells stably transfected with siNC, siLINC01094#1 and siLINC01094#2 (**p<0.01). (C-D) LINC01094 knockdown decreased cell viability and colony formation capacity in PANC-1 cells (**p<0.01, scale bar, 100 μm). (E) Western blot to detect proliferation-associated antigen PCNA expression in PANC-1 and ASPC-1 cells stably transfected with siNC, siLINC01094#1 and siLINC01094#2 (**p<0.01); data were expressed as mean±SD and analyzed using unpaired t-test. The experiment was repeated three times.
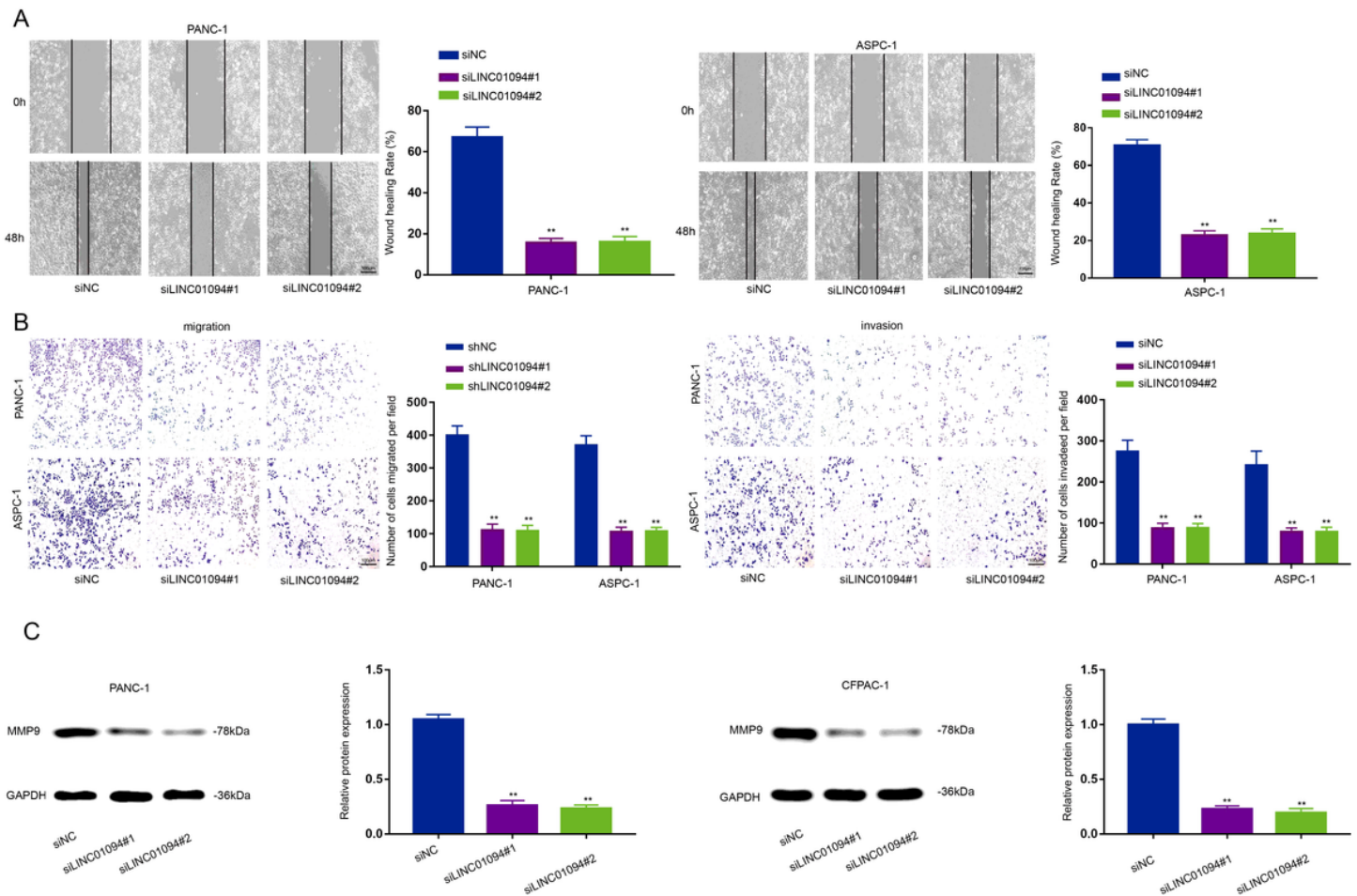
Figure 3

LINC01094 promotes PC cell metastasis in vitro. (A-B) metastasis ability was measured using wound healing and transwell assays in PC cells transfected with siNC, siLINC01094#1 and siLINC01094#2 (**p<0.01, scale bar, 100 μm). (C) Western blot to detect proliferation-associated antigen MMP9 expression in PANC-1 and ASPC-1 cells stably transfected with siNC, siLINC01094#1 and siLINC01094#2 (**p<0.01); data were expressed as mean±SD and analyzed using unpaired t-test. The experiment was repeated three times.
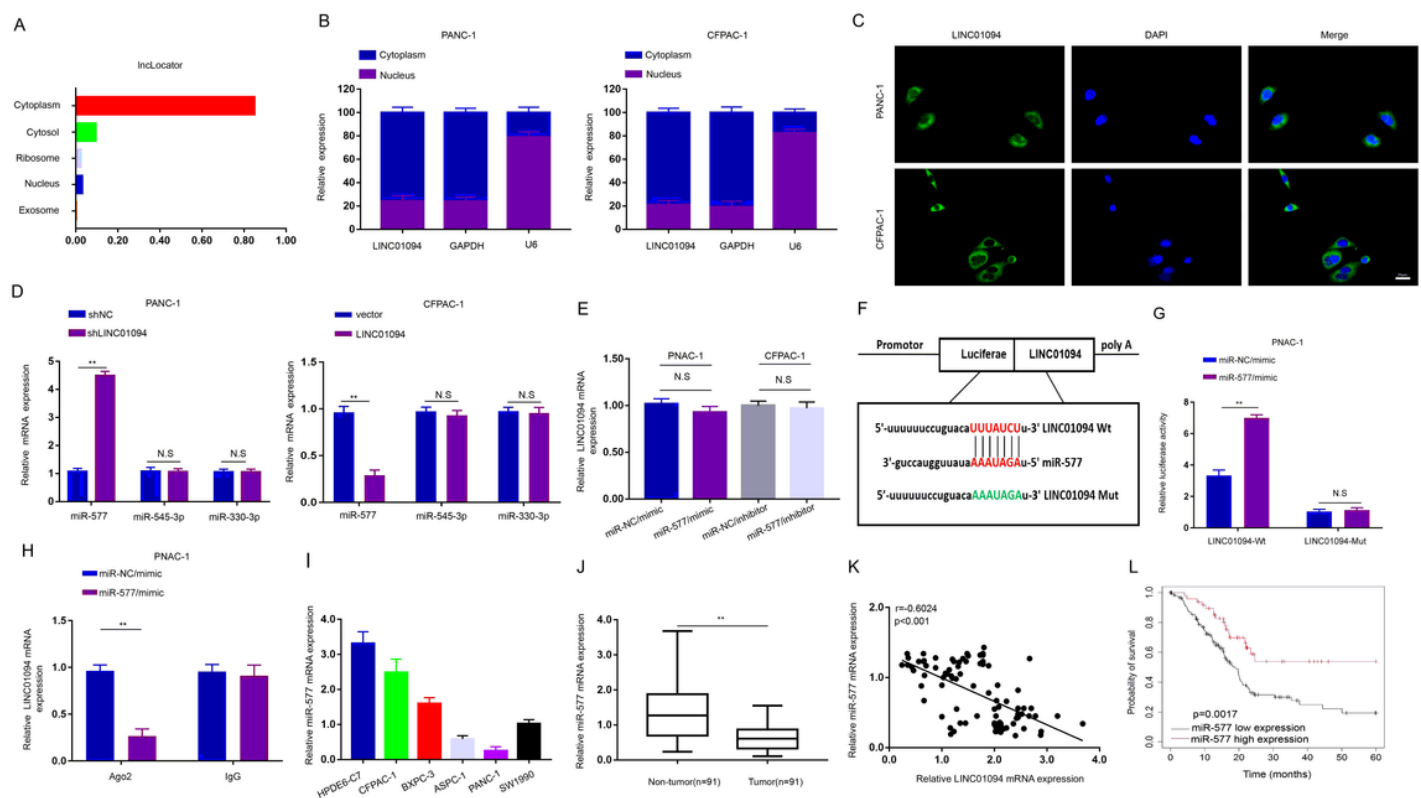
Figure 4

LINC01094 acts as miRNA sponge for miR-577. (A-B) LINC01094 localization was predicted using lncRNA subcellular localization predictor, lncLocator. (C) Fluorescence in situ hybridization (FISH) assay was conducted to determine the subcellular localization of LINC01094 in PANC-1 cells. Nuclei are stained blue (DAPI), and LINC01094 is stained green (Scale bars, 25 μm). (D) Three miRNAs were predicted from starBase and the expression levels of the three miRNAs were detected in cells transfected with LINC01094 expression vector or shLINC01094 (**$p<0.01$; NS, not significant). (E) The expression of LINC01094 were analyzed in cells stably transfected with miR-577/mimic or miR-577/inhibitor (**$p<0.01$; NS, not significant). (F) The putative miR-577 binding sites with the LINC01094 sequence 3'-UTR are shown. (G) Luciferase activity in PANC-1 cells co-transfected with miR-NC/mimic and miR-577/mimic containing LINC01094-Wt and LINC01094-Mut. (H) RNA-IP with anti-antibodies was performed in PANC-1 cells transfected with miR-NC/mimic and miR-577/mimic (**$p<0.01$; NS, not significant). (I) miR-577 mRNA expression was analyzed in the PC cells and a normal pancreatic cell. (J) The expression levels of miR-577 in 91 pairs of PC and in adjacent non-tumor tissues, (** $p<0.01$). (K) Scatter plots show a positive correlation between LINC01094 and miR-577 at the mRNA levels in 91 PC tissues (r=-0.6024, *$p<0.05$, **$p<0.01$). (L) Kaplan-Meier analysis of survival time with miR-577 high and low level in PC patients from TCGA database (p=0.0017); those among multiple groups were analyzed by the one-way ANOVA or repeated-measures ANOVA. Correlation analysis between two groups was conducted using Pearson's correlation analysis. The experiment was repeated three times.

Figure 5

LIN28B is a downstream target of miR-577. (A) Potential targets of miR-577 predicted with five miRNA target databases. (B) qRT-PCR analysis for the 4 predicted targets of miR-577 in PANC-1 cells transfected with miR-577/mimics (**p<0.01; NS, not significant). (C) The putative miR-577 binding sites with the LIN28B sequence 3'-UTR were shown. (D) Luciferase reporter gene activity of chimeric vectors carrying luciferase gene and LIN28B 3'-UTR fragments containing Wt-LIN28B or Mut-LIN28B binding sites

(**p<0.01; NS, not significant). (E), LIN28B mRNA and protein expression were analyzed in PANC-1 and CFPAC-1 cells transfected with miR-577/mimic and miR-577/inhibitor (**p<0.01). (F) Western blot to detect proliferation-associated antigen PCNA, MMP9 and LIN28B expression in PC cells stably transfected with miR-NC/inhibitor and miR-577/mimic and miR-NC/inhibitor and miR-577/mimi (**p<0.01). (G-H) PC cells proliferation were measured using clone formation and EdU assays in PC cells transfected with the miR-NC/inhibitor and miR-577/mimic (**p<0.01, scale bar, 100 μm). (I-J) PC cells invasion and migration were measured through wound healing and transwell assays in PC cells transfected with the miR-NC/inhibitor and miR-577/mimic (**p<0.01, scale bar, 100 μm). (K) The elevated expression of LIN28B in tissue level was detected by IHC test, normalized to pancreatic cancer tissue group (**p<0.01, scale bar, 100 μm). (L) Scatter plots show a positive correlation between LINC01094 and LIN28B at the mRNA levels in 91 PC tissues (r=0.4918, **p<0.01); those among multiple groups were analyzed by the one-way ANOVA or repeated-measures ANOVA. Correlation analysis between two groups was conducted using Pearson's correlation analysis. The experiment was repeated three times, (mean ± SEM).
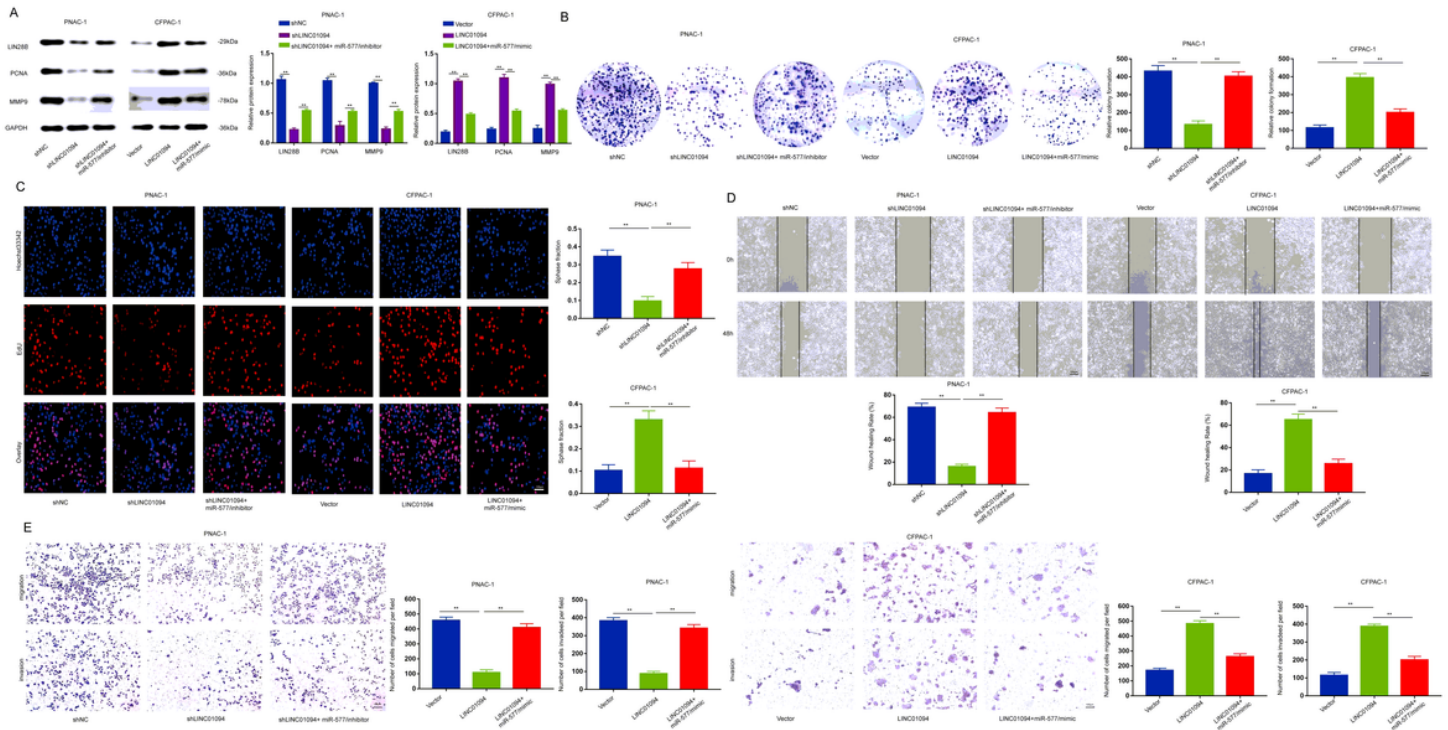

Figure 6

LINC01094 acts as a sponge of miR-577 to upregulating LIN28B expression. (A) Western blotting analysis of proliferation-associated antigens in PANC-1 and CFPAC-1 cells stably transfected with shNC, shLINC01094, shLINC01094+miR-577/inhibitor and vector, LINC01094, LINC01094+miR-577/mimic. (B-C) Clone formation and EdU assays was performed to determine the mobility capacity of PANC-1 and CFPAC-1 cells stably transfected with shNC, shLINC01094, shLINC01094+miR-577/inhibitor and vector, LINC01094, LINC01094+miR-577/mimic (**p<0.01, scale bar, 100 μm). (D-E) Wound healing and transwell assays was performed to determine the mobility capacity of PANC-1 and CFPAC-1 cells stably

transfected with shNC, shLINC01094, shLINC01094+miR-577/inhibitor and vector, LINC01094, LINC01094+miR-577/mimic (**p<0.01, scale bar, 100 μm); those among multiple groups were analyzed by the one-way ANOVA or repeated-measures ANOVA. The experiment was repeated three times, (mean ± SEM).
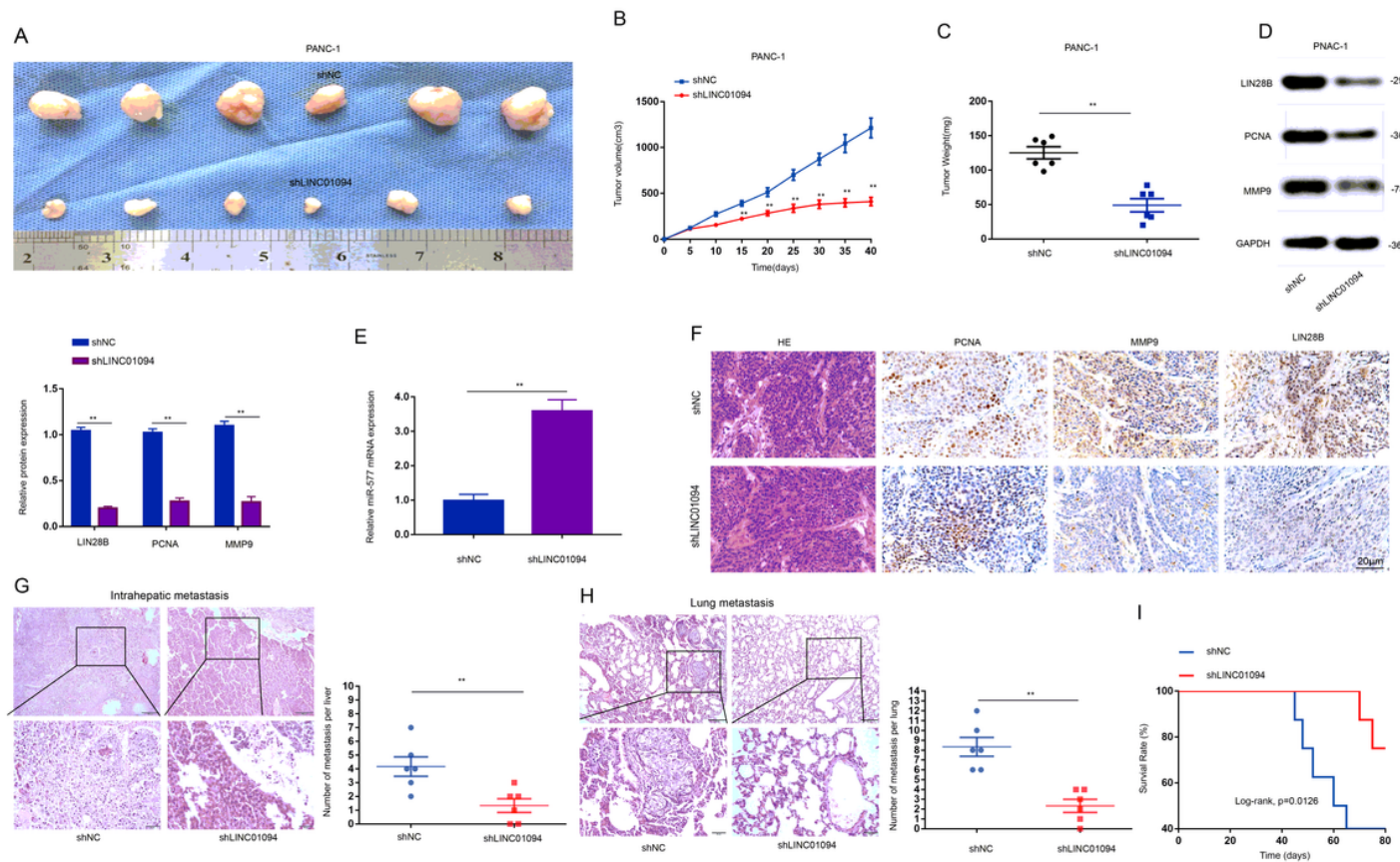

Figure 7

Silencing of LINC01094 suppresses the proliferation and metastasis of PC cells in vivo. (A) Forty days after injection, the nude mice were killed and the tumors in each group were shown. (B-C) The tumor growth curve was observed after subcutaneous injection of PNAC-1 cells expressing shNC or shLINC01094 , and the tumor weight and volume were measured in mouse xenografts. (mean ± SEM, n=6, **p<0.01, scale bar, 100 μm), data are representative of at least three independent experiments. (D) Relative expression levels of MMP9, PNCA and LIN28B are observed in subcutaneous tumor tissues by western blot assays. (E) PANC-1-tumor samples from shNC and shLINC01094-treated mice were analyzed by qRT-PCR (**p<0.01). (F) PANC-1-tumor samples from shNC and shLINC01094-treated mice were immunohistochemically stained for LIN28B, MMP9 and PCNA (Scale bars, 20 μm). (G-H) Sections with metastatic nodules in the liver and lung were stained with H&E, the number of metastatic nodules was analyzed (**p<0.01, scale bar, 100 μm), (I) Kaplan-Meier survival curves for mice of the PANC-1-shLINC01094 group and control group (p=0.00126); data were expressed as mean±SD and analyzed using unpaired t-test. The experiment was repeated three times.

Supplementary Files

This is a list of supplementary files associated with this preprint. Click to download.

- SupplementaryTable1.docx
- SupplementaryTable2.docx
- SUPPFigure.1.tif
- SUPPFigure.2.tif
- SUPPFigure.3.tif
- SUPPFigure.4.tif
- SUPPFigure.5.tif
- SUPPFigure.6.tif